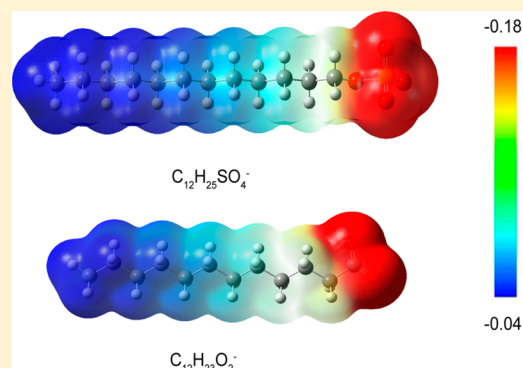


Self-Aggregation of New Alkylcarboxylate-Based Anionic Surface Active Ionic Liquids: Experimental and Theoretical Investigations

Ni Cheng,[†] Pengming Yu,[‡] Tao Wang,[§] Xiang Sheng,[†] Yanhui Bi,[†] Yanjun Gong,[†] and Li Yu^{*,†}[†]Key Laboratory of Colloid and Interface Chemistry, Shandong University, Ministry of Education, Jinan 250100, PR China[‡]China Research Institute of Daily Chemical Industry, Taiyuan 030001, PR China[§]Production Technology Institute, Shengli Oilfield, Dongying 257000, PR China

ABSTRACT: Halogen-free and low-cost alkylcarboxylate-based anionic surface active ionic liquids (SAILs), namely, 1-butyl-3-methylimidazolium alkylcarboxylates ($[\text{C}_4\text{mim}][\text{C}_n\text{H}_{2n-1}\text{O}_2]$, $n = 8, 10, 12$), were first synthesized through the neutralization of imidazolium hydroxide by alkylcarboxylic acids. A systematic study of their self-aggregation behavior in water was investigated by surface tension, electrical conductivity, steady-state fluorescence quenching, and ^1H NMR. The micellar properties of this series of SAILs in ethylammonium nitrate (EAN) were also studied by surface tensiometry for comparison. A set of surface active parameters and thermodynamic parameters of these compounds in water and EAN was obtained. Surface tension results show that the surface activity of $[\text{C}_4\text{mim}][\text{C}_n\text{H}_{2n-1}\text{O}_2]$ in EAN is inferior to that in water. They exhibit a higher ability to aggregate in water than the traditional anionic surfactants, sodium alkylcarboxylates (SAC), and anionic SAILs, 1-butyl-3-methylimidazolium alkylsulfates ($[\text{C}_4\text{mim}][\text{C}_n\text{H}_{2n+1}\text{SO}_4]$) with the same hydrocarbon chain length. This demonstrates that the incorporation of carboxylate group and $[\text{C}_4\text{mim}]^+$ cation favors micelle formation. To understand the discrepancy in the surface activity of alkylsulfate- and alkylcarboxylate-based SAILs, theoretical calculations were performed to give electrostatic potential of the corresponding anions. The higher surface activity of $[\text{C}_4\text{mim}][\text{C}_{12}\text{H}_{23}\text{O}_2]$ mainly originates from the lower electronegativity of its anion. Density functional theory (DFT) calculations manifest that the interaction energy of binary combination SAILs–EAN is larger than that of SAILs– H_2O , implying the stronger interaction of the former. Consequently, it is more difficult for $[\text{C}_4\text{mim}][\text{C}_n\text{H}_{2n-1}\text{O}_2]$ to self-aggregate in EAN than in H_2O . This work is expected to be of practical value for the environmentally friendly alkylcarboxylate-based SAILs in some potential applications, including nanomaterials synthesis and phase separation, among others.



■ INTRODUCTION

Ionic liquids (ILs) are a class of organic salts that are liquids below 100 °C, and they have attracted much attention for their specific chemical and physical properties.¹ There exist over 225 types of ILs which have been widely investigated as electrolytes and as a green solvent for catalyst and extraction.² The great advantage of ILs is that their physicochemical properties can be designed by a reasonable selection of cations, anions, and substituents.³ The inherent amphiphilic character of some ILs with long alkyl chains has yielded surface-active properties that are usually better than those of traditional surfactants. Thus, they have emerged as a novel kind of amphiphile and known as surface active ionic liquids (SAILs).⁴ In recent years, most of the investigations in this field are focused on the formation of SAILs aggregates in water.^{5–12} By changing the alkyl chain length, the type of headgroup, and the nature of counterions, one can modify their aggregation behavior.^{13–15} Of particular interest in this regard is SAILs composed of the 1-alkyl-3-methyl-imidazolium cation C_nmim^+ , where n is the carbon number of alkyl chain.^{10,16–18}

Apart from the studies on the molecular assemblies of SAILs in aqueous solution, their aggregation in room-temperature ionic liquids (RTILs) has also attracted much attention recently. This kind of pure ionic liquid system may have some advantages such as high thermal stability and fine-tuning properties due to the waterless and nonvolatile nature.¹⁹ Ethylammonium nitrate (EAN) has the potential to build up hydrogen-bonding networks like water due to its protic nature and general solvent properties, which is postulated to support self-assembly.²⁰ Kang et al. investigated the aggregation behavior and micelle formation mechanism of 1-alkyl-3-methyl-imidazolium bromides ($[\text{C}_n\text{mim}]\text{Br}$) in EAN by analyses of ^1H NMR spectrum and thermodynamic data. They found that the micelle formation for $[\text{C}_n\text{mim}]\text{Br}$ in EAN is more favorable than that in bmimBF_4 but more difficult than that in aqueous solution.²¹ Kunz et al. presented the results on the colloidal characteristics of 1-hexadecyl-3-methyl-imidazo-

Received: December 18, 2013

Revised: February 17, 2014

Published: February 20, 2014

lium bromide ($[\text{C}_{16}\text{mim}]\text{Br}$)/EAN and 1-hexadecyl-3-methylimidazolium tetrafluoroborate ($[\text{C}_{16}\text{mim}]\text{BF}_4$)/EAN and confirmed that the SAILs/IL mixtures were stable at temperature up to 250 °C or so.¹⁹ Shi et al. explored the aggregation behavior of *N*-alkyl-*N*-methylpyrrolidinium bromides (C_nMPB , $n = 12, 14, 16$) in EAN. They demonstrated that some ethylammonium cations might be incorporated into the head groups and behave as cosurfactants.²²

Currently, due to the sustainable development of chemicals, some vital issues such as biodegradability, stability, and the lifecycle of SAILs have been intensively investigated.^{23,24} However, almost all the SAILs studied have halogen atoms situating on the anions, where the presence of halogen atoms (such as Cl or F) might release HCl or HF by hydrolysis under certain conditions and lead to serious concerns such as environmental hazards and toxicity. In recent years, several greener amphiphiles based on the structures of ILs have emerged, for instance, amino acid-²⁵ and imidazolium-based alkylsulfate SAILs free of halogen.^{9,11,12,26} Kumar's group synthesized novel amino-acid-based SAILs with better surface activity than conventional surfactants and demonstrated their potential applications in areas such as the mitigation of harmful algal blooms from seawater and the shape- and size-specific synthesis of nanomaterials.²⁵ They also observed dual transitions in the physical properties of 1-butyl-3-methylimidazolium octylsulfate ($[\text{C}_4\text{mim}][\text{C}_8\text{H}_{17}\text{SO}_4]$) aqueous solution: the first transition corresponds to anionic aggregation, and the second transition is restructuring of the anionic aggregates to a peculiar structure.⁹ Our group carried out a detailed study of the aggregation behavior of halogen-free SAILs, 1-butyl-3-methylimidazolium dodecylsulfate ($[\text{C}_4\text{mim}][\text{C}_{12}\text{H}_{25}\text{SO}_4]$) and *N*-butyl-*N*-methylpyrrolidinium dodecylsulfate ($[\text{C}_4\text{MP}][\text{C}_{12}\text{H}_{25}\text{SO}_4]$) in water.²³ Compared to the attention received by imidazolium-based ILs with alkylsulfate anion, there are very few reports on imidazolium salts functionalized with carboxylic ester group. Zhuo et al. prepared a class of 1-butyl-3-methylimidazolium carboxylate ionic liquids ($[\text{C}_4\text{mim}][\text{HCOO}]$, $[\text{C}_4\text{mim}][\text{CH}_3\text{COO}]$ and $[\text{C}_4\text{mim}][\text{CH}_3\text{CH}_2\text{COO}]$) and studied the interaction characteristics of them with glucose in aqueous solution.²⁷ However, so far the aggregation behavior of SAILs bearing alkylcarboxylate anion has not been studied. This paper describes the straightforward synthesis of halogen-free imidazolium alkylcarboxylates ($[\text{C}_4\text{mim}][\text{C}_n\text{H}_{2n-1}\text{O}_2]$, $n = 8, 10, 12$) using some inexpensive chemicals and detailed studies of the self-aggregation behaviors of these SAILs in water and EAN by various techniques. In comparison with the corresponding conventional ionic surfactants, SAC, and imidazolium-based SAILs, $[\text{C}_4\text{mim}][\text{C}_n\text{H}_{2n+1}\text{SO}_4]$, the special nature of imidazolium-based alkylcarboxylate SAILs has been studied. The effects of hydrocarbon chain length on the anion and type of solvent on the self-aggregation behavior of this kind of SAILs have been investigated.

EXPERIMENTAL SECTION

Materials. 1-Methylimidazole (99%) was purchased from Acros Organics. 1-Chlorobutane (98%) and alkylcarboxylic acids (98%) were obtained from Shanghai Aladdin Chemistry Co., Ltd. of China. Pyrene (99%) was purchased from Alfa Aesar. D_2O (99.9%) and CDCl_3 (99.9%) were bought from Sigma-Aldrich. All the reagents were used without further purification. Triply distilled water was used to prepare all the solutions.

Apparatus and Procedures. Surface tension measurements were carried out on a model JYW-200B tensiometer (Chengde Dahua Instrument Co., Ltd., accuracy ± 0.1 mN/m) using the ring method. The surface tension was determined with single-measurement mode. Electrical conductivity measurements were employed on a low frequency conductivity analyzer (model DDSJ-308A, Shanghai Precision & Science Instrument Co., Ltd. of China). Each conductivity was recorded when its stability was better than 1% within 2 min. The temperature of both surface tension and electrical conductivity measurements was controlled by a thermostatic water bath, and the uncertainty was within ± 0.1 °C.

The steady-state fluorescence measurements were taken using a Perkin-Elmer fluorimeter LS-55. Pyrene was used as a fluorescent probe. The pyrene-containing solution was collected with a 1 cm³ quartz cuvette. The fluorescence excitation wavelength was focused at 335 nm, the emission wavelength ranged from 350 to 500 nm, and slit widths for emission and excitation were fixed at 2 and 10 nm, respectively. The pyrene concentration was kept at 1×10^{-6} mol·L⁻¹ to avoid excimer formation in all the measurements. All the fluorescence spectral measurements were conducted at 25 ± 0.1 °C.

¹H NMR spectra were carried out with a Bruker Avance 400 spectrometer at the frequency of 400 MHz at 25 ± 0.1 °C. Reproducibility of the results was confirmed by performing at least two experiments for each sample. Uncertainty for the chemical shift values was less than 10^{-3} ppm.

Synthesis of Ionic Liquids. 1-Butyl-3-methylimidazolium chloride ($[\text{C}_4\text{mim}]\text{Cl}$) was freshly prepared in our laboratory according to the procedures reported previously.²³ An aqueous solution of $[\text{C}_4\text{mim}]\text{Cl}$ was allowed to pass through a column filled with anion exchange resin to obtain $[\text{C}_4\text{mim}][\text{OH}]$.²⁸ This reaction progress was tested by AgNO_3 . When chloride ions were completely replaced by hydroxide ions, no precipitation of AgCl could be found. 1-Butyl-3-methylimidazolium alkylcarboxylates ($[\text{C}_4\text{mim}][\text{C}_n\text{H}_{2n-1}\text{O}_2]$, $n = 8, 10, 12$) (with the chemical structures represented in Figure 1) were

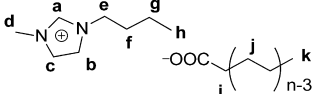
SAILs	Abbreviations
	$n=8, [\text{C}_4\text{mim}][\text{C}_8\text{H}_{15}\text{O}_2]$
	$n=10, [\text{C}_4\text{mim}][\text{C}_{10}\text{H}_{19}\text{O}_2]$
	$n=12, [\text{C}_4\text{mim}][\text{C}_{12}\text{H}_{23}\text{O}_2]$

Figure 1. Chemical structures of the synthesized SAILs and their abbreviations.

obtained by the neutralization of $[\text{C}_4\text{mim}]\text{OH}$ and the corresponding alkylcarboxylic acids following the similar procedure. The aqueous $[\text{C}_4\text{mim}][\text{OH}]$ solution and equal moles of the alkyl fatty acid were stirred in a flask at 40 °C for 10 h. After removing water by evaporation under reduced pressure, the viscous liquid was finally dried under vacuum at 60 °C for 72 h. Structures of the resulting ionic liquids were confirmed by ¹H NMR spectroscopy with a Bruker Avance 300 spectrometer in CDCl_3 , and the ¹H NMR peak of CDCl_3 (7.26 ppm) was used as the reference in determining the proton chemical shifts. For $[\text{C}_4\text{mim}][\text{C}_8\text{H}_{15}\text{O}_2]$, 11.00 (s, 1H, NCHN), 7.29, 7.18 (ss, 2H, NCH), 4.30 (t, 2H, NCH_2), 4.06 (s, 3H, NCH_3), 2.24 (t, 2H, COCH_2) 1.86 (m, 2H, NCCCH_2), 1.60 (m, 2H, NCCCH_2), 1.34 (m, $\text{COCH}_2(\text{CH}_2)_5$,

10H), 0.96 (t, 3H, NCCCCH₃), 0.86 (t, 3H, COC₆CH₃). [C₄mim][C₁₀H₁₉O₂], ¹H NMR (δ/ppm): 11.38 (s, 1H, NCHN), 7.28, 7.12 (ss, 2H, NCH), 4.30 (t, 2H, NCH₂), 4.07 (s, 3H, NCH₃), 2.25 (t, 2H, COCH₂) 1.86 (m, 2H, NCCH₂), 1.62 (m, 2H, NCCCCH₂), 1.36 (m, COCH₂(CH₂)₇, 14H), 0.96 (t, 3H, NCCCCH₃), 0.87 (t, 3H, COC₈CH₃). [C₄mim][C₁₂H₂₃O₂] 11.00 (s, 1H, NCHN), 7.25, 7.17 (ss, 2H, NCH), 4.32 (t, 2H, NCH₂), 4.07 (s, 3H, NCH₃), 2.24 (t, 2H, COCH₂) 1.89 (m, 2H, NCCH₂), 1.61 (m, 2H, NCCCCH₂), 1.35 (m, COCH₂(CH₂)₉, 18H), 0.96 (t, 3H, NCCCCH₃), 0.87 (t, 3H, COC₁₀CH₃).

RESULTS AND DISCUSSION

Surface Properties and Micellization Parameters.

Surface tension values of the synthesized SAILs in both water and EAN were measured in order to evaluate their surface activity. The variations of the surface tension (γ) at 25 °C

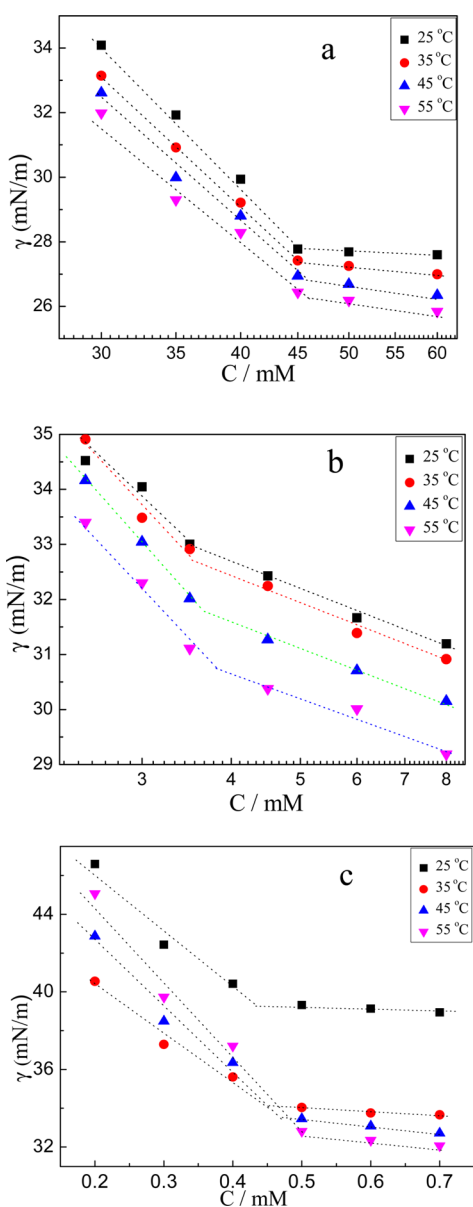


Figure 2. Plots of surface tension versus concentration for [C₄mim]-[C_nH_{2n-1}O₂] in water at different temperatures: (a) *n* = 8; (b) *n* = 10; (c) *n* = 12.

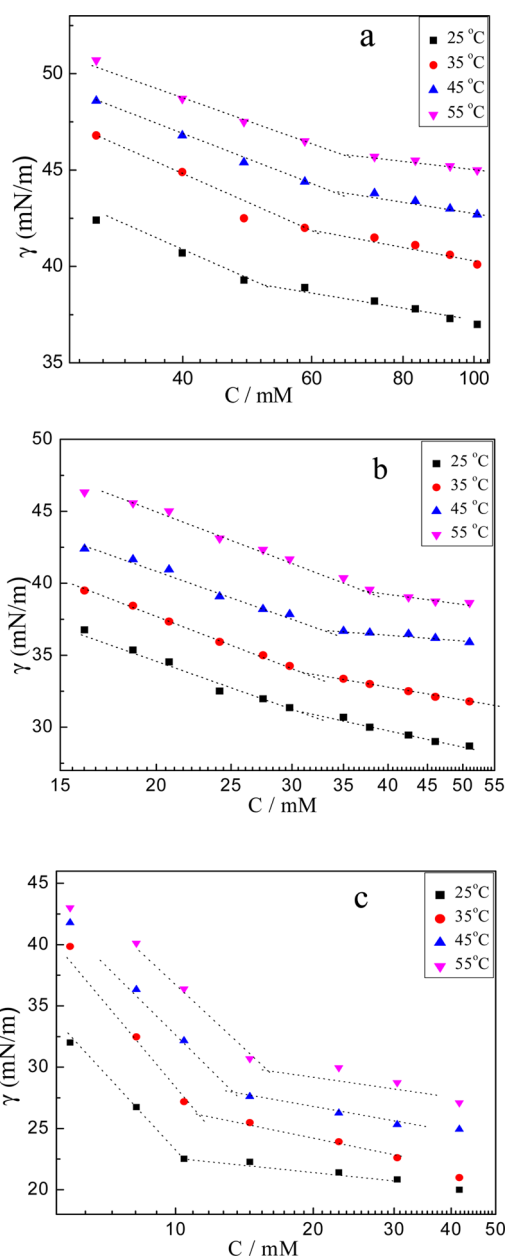


Figure 3. Plots of surface tension versus concentration for [C₄mim]-[C_nH_{2n-1}O₂] in EAN at different temperatures: (a) *n* = 8; (b) *n* = 10; (c) *n* = 12.

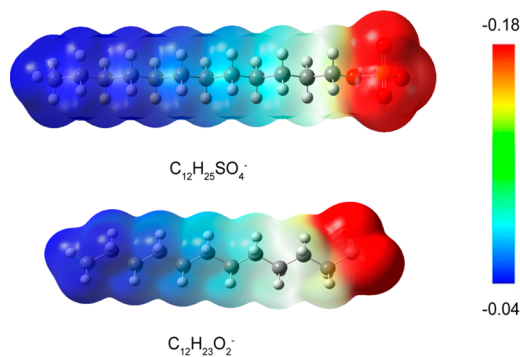
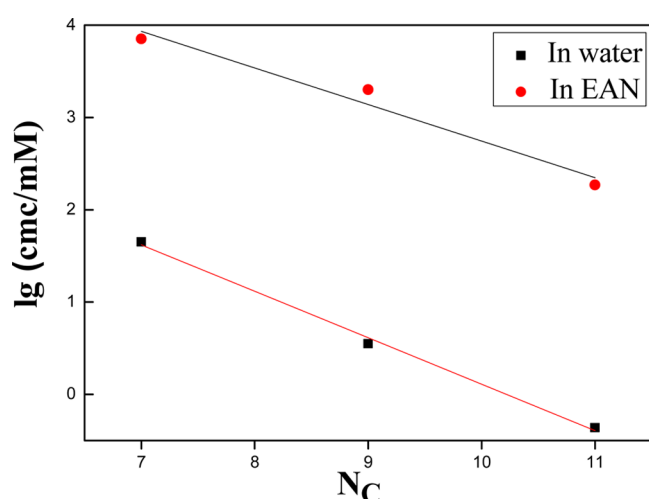


Figure 4. B3LYP/6-31G (d,p) electrostatic potentials, in Hartrees, at the 0.001 e/bohr³ isodensity surfaces of C₁₂H₂₅SO₄⁻ and C₁₂H₂₃O₂⁻ anions.

Table 1. Surface Property Parameters of Alkylcarboxylate Based SAILs in Both Water and EAN, Alkylsulfate based SAILs, and SAC in Water at 25 °C

	<i>n</i>	cmc (mM)		γ_{cmc} (mN/m)	A_{min} (Å ²)	Γ_{max} (μmol/m ²)
[C ₄ mim][C _{<i>n</i>} H _{2<i>n</i>-1} O ₂] (in water)	8	45.0 ^a	42.2 ^b	44.9 ^c	27.8	53.3
	10	3.54	3.42	3.55	36.8	49.6
	12	0.44		0.45	39.3	60.3
[C ₄ mim][C _{<i>n</i>} H _{2<i>n</i>-1} O ₂] (in EAN)	8	47.1			39.0	93.6
	10	27.2			31.3	81.0
	12	9.66			22.5	44.3
[C ₄ mim][C _{<i>n</i>} H _{2<i>n</i>+1} SO ₄] ^d (in water)	10	8.8			34.7	59
	12	1.9			33.8	66
SAC ^e (in water)	8	340.0				
	10	94.0				
	12	24.4				

^aFrom surface tension measurements. ^bFrom steady state fluorescence measurements. ^cFrom electrical conductivity measurements. ^dReported in ref 33. ^eReported in ref 34.

**Figure 5.** Variation of lg cmc with the carbon number of hydrophobic chain for [C₄mim][C_{*n*}H_{2*n*-1}O₂] (*n* = 8, 10, 12) at 25 °C.

versus concentration (*C*) for [C₄mim][C_{*n*}H_{2*n*-1}O₂] (*n* = 8, 10, 12) are represented in Figures 2 and 3. From these data, it is apparent [C₄mim][C_{*n*}H_{2*n*-1}O₂] behave just as classical surfactants in water^{22,23} or EAN.^{29–31} The surface tension decreases initially with increasing [C₄mim][C_{*n*}H_{2*n*-1}O₂] concentration up to a plateau region, above which a nearly constant value of surface tension (γ_{cmc}) is observed. This result suggests that solvophobic interactions exist between EAN and the hydrocarbon chain of the imidazolium-based SAILs, similar to the hydrophobic interactions in water.³² A noteworthy fact is the absence of a minimum around the breakpoint, confirming the high purities of these prepared products. The break point between the two regions on the line is assigned to the critical micelle concentration (cmc) value. The estimated cmc and γ_{cmc} values for [C₄mim][C_{*n*}H_{2*n*-1}O₂] (*n* = 8, 10, 12) are listed in Table 1, together with those data reported for 1-butyl-3-methylimidazolium alkylsulfates ([C₄mim][C_{*n*}H_{2*n*+1}SO₄], *n* = 10, 12)³³ and corresponding sodium alkylcarboxylates (SAC, *n* = 8, 10, 12)³⁴ which have the same hydrophobic chain length.

Table 1 shows that the cmc value of [C₄mim][C_{*n*}H_{2*n*-1}O₂] in water is notably smaller than that of sodium carboxylate with the same hydrophobic chain length by 1 or 2 orders of magnitude, suggesting that the SAILs synthesized in this work have a more prominent surface activity. It can be attributed to the more effective screening for intramolecular electrostatic

repulsions offered by [C₄mim]⁺ cation, due to the easier adsorption on the micellar surface in the Stern layer compared to Na⁺. This decreases the charge repulsion between polar head groups, facilitating the formation of micelles.⁵ Moreover, the higher hydrophobicity of [C₄mim]⁺ cation is considered to result in the lower cmc values of these SAILs.⁵ In addition, the cmc values of [C₄mim][C_{*n*}H_{2*n*-1}O₂] in water are smaller than those of the corresponding alkylsulfate-based SAILs, [C₄mim]-[C_{*n*}H_{2*n*+1}SO₄], which can be ascribed mainly to the difference of the anions. For better understanding the electrostatic interaction between the polar headgroup for the SAILs based on alkylcarboxylate or alkylsulfate anion, quantum chemistry calculations were carried out. All of the density functional theory (DFT) calculations in this work were implemented by the Gaussian09 package³⁵ using the B3LYP^{36–38} functional with the standard 6-31G(d,p) basis set.^{39,40} Frequency calculations were performed to verify that all the optimized geometries correspond to a local minimum that has no imaginary frequency. Figure 4 depicts the electrostatic potentials at the 0.001 e/bohr³ isodensity surfaces of C₁₂H₂₅SO₄[−] and C₁₂H₂₃O₂[−] anions. It is obvious that both the headgroups of the two anions are electronegative. The less electronegative C₁₂H₂₃O₂[−] anion means that its electrostatic repulsion is weaker than that of C₁₂H₂₅SO₄[−] anion, which primarily accounts for the lower cmc value of [C₄mim]-[C₁₂H₂₃O₂].

The maximum surface excess concentration (Γ_{max}) and the occupied area per surfactant molecule (A_{min}) reflect the arrangement of surfactant molecules at the air–liquid interface. According to Gibbs Law,⁴¹ Γ_{max} can be calculated by the following equation

$$\Gamma_{\text{max}} = -\frac{1}{nRT} \left(\frac{d\gamma}{d \ln C} \right)_T \quad (1)$$

where *n* represents the number of species constituting the surfactant which are adsorbed at the interface. Here, *n* is taken to be equal to 2. The A_{min} value can be obtained from

$$A_{\text{min}} = \frac{1}{\Gamma_{\text{max}} N_A} \times 10^{24} \quad (2)$$

where N_A is Avogadro's number ($6.02 \times 10^{23} \text{ mol}^{-1}$). Table 1 summarizes the Γ_{max} and A_{min} values for [C₄mim][C_{*n*}H_{2*n*-1}O₂] (*n* = 8, 10, 12), along with those data of [C₄mim][C_{*n*}H_{2*n*+1}SO₄] (*n* = 10, 12) reported previously.³³ It is well-documented that

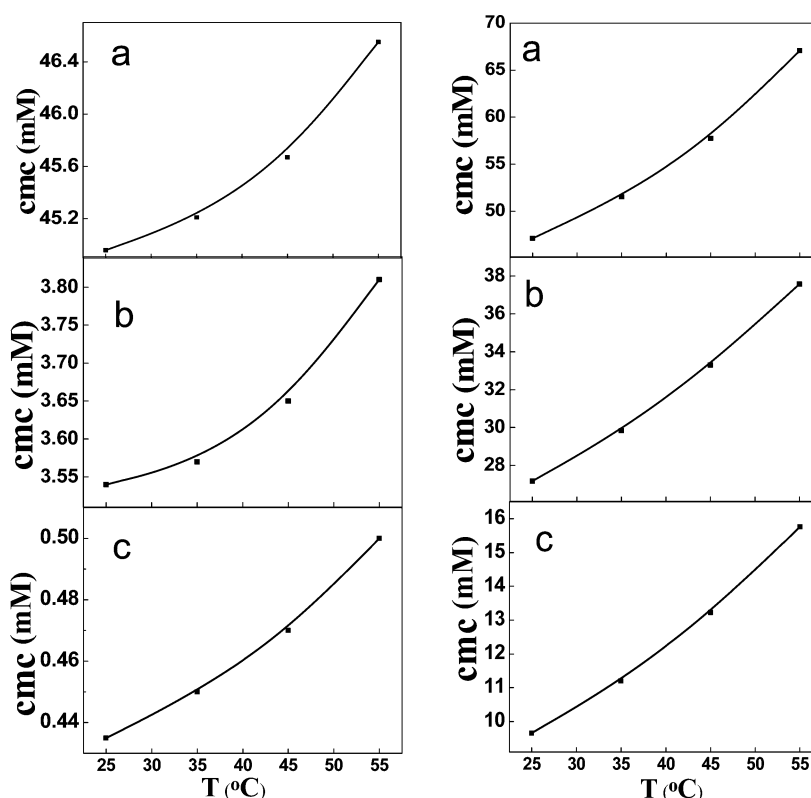


Figure 6. Plots of cmc values obtained by surface tension measurements against temperature for $[C_4mim][C_nH_{2n-1}O_2]$ in water (left) and in EAN (right): (a) $n = 8$; (b) $n = 10$; (c) $n = 12$.

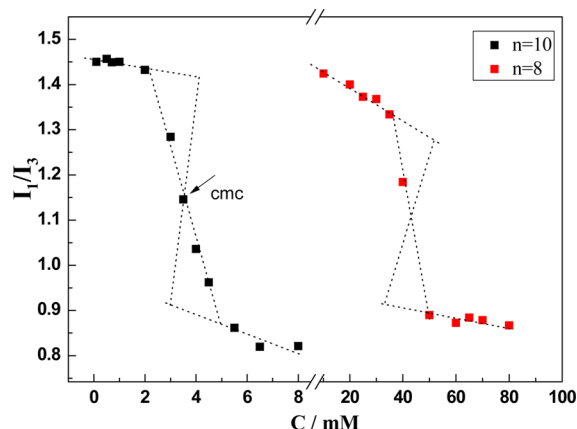


Figure 7. Variation of I_1/I_3 ratio of pyrene versus concentration of $[C_4mim][C_nH_{2n-1}O_2]$ at 25 °C.

the structure of the hydrophilic headgroup is a dominant factor influencing the adsorption of surfactant at the air–liquid interface.⁴² By replacing SO_4^- with COO^- , we observe a larger Γ_{max} and smaller A_{min} values for $[C_4mim][C_nH_{2n-1}O_2]$, which signifies a denser arrangement of the alkylcarboxylate-based SAIL molecules at the air–water interface, compared to alkylsulfate-based SAIL.⁴³ The van der Waals volumes⁴⁴ calculated with default electron density isosurface (0.001 e/bohr³) are 221.71 and 189.01 cm³/mol for $C_{12}H_{25}SO_4^-$ and $C_{12}H_{23}O_2^-$ anions, respectively. The smaller size and reduced electronegativity (Figure 4) of the polar headgroup shown by the results of quantum chemistry calculations can be used to interpret the closer arrangement of $[C_4mim][C_nH_{2n-1}O_2]$ molecules at the air–water interface.

For a homologous series of linear single-chain amphiphiles, the cmc value decreases logarithmically with the carbon number of alkyl chain, following the empirical Klevens equation⁴⁵

$$\lg \text{cmc} = A - BN_c \quad (3)$$

where A and B are constants in particular homologous series at constant temperature. The A value reflects the contribution of the polar headgroup to micelle formation, and B measures the effect of each additional methylene group in the hydrophobic chain on cmc. A smaller magnitude of A or a larger magnitude of B implies that micelle formation is more favorable. Figure 5 gives the correlation between cmc and the number of carbon atoms (N_c) in the hydrocarbon chain for $[C_4mim][C_nH_{2n-1}O_2]$ ($n = 8, 10, 12$) at 25 °C, and the values of A and B obtained are 5.64 and 0.50 in water, 7.10 and 0.40 in EAN, respectively. This result indicates that the ability for $[C_4mim][C_nH_{2n-1}O_2]$ to form micelles in water is superior to that in EAN.

The surface tension values of $[C_4mim][C_nH_{2n-1}O_2]$ ($n = 8, 10, 12$) in both water and EAN at other temperatures were also determined, and the curves of surface tension versus concentration are depicted in Figures 2 and 3, respectively. Figure 6 represents the plots of cmc in the two kinds of solvents as a function of temperature. It is evident that the cmc values increase as the temperature rises, and the increasing tendency can fit a second-order polynomial, similar to the tendencies of traditional ionic surfactants in water or ionic liquid.^{22,46} It is well-known that when the temperature increases the order structure of water molecules surrounding the hydrophobic domain is destroyed, which is unfavorable to micellization, and then cmc increases. An analogous mechanism

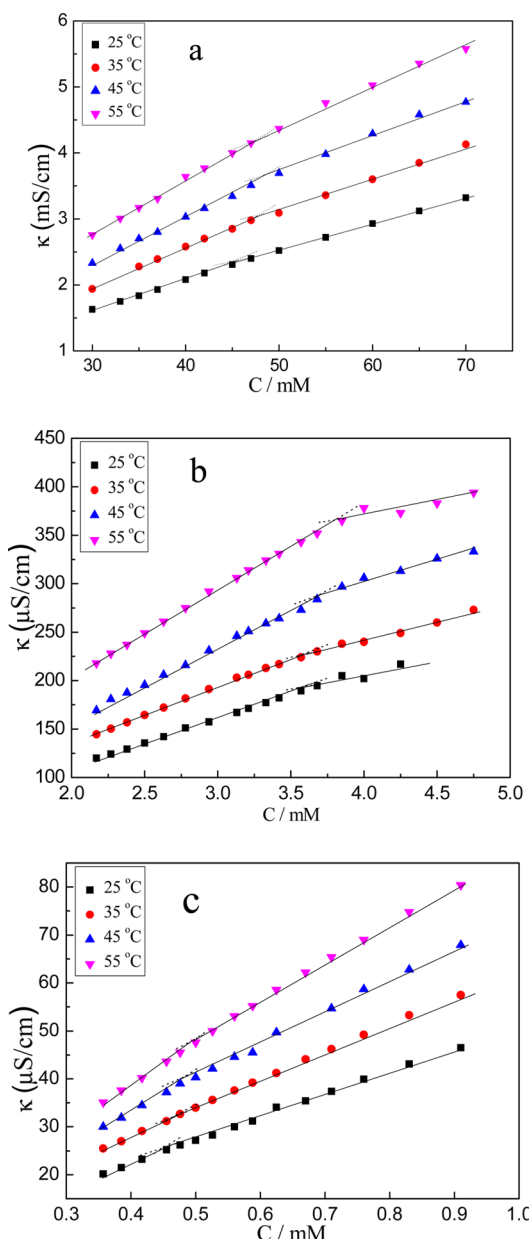


Figure 8. Plots of electrical conductivity versus concentration of $[C_4mim][C_nH_{2n-1}O_2]$ in water at 25 °C: (a) $n = 8$; (b) $n = 10$; (c) $n = 12$.

can be used to interpret the self-aggregation of $[C_4mim]-[C_nH_{2n-1}O_2]$ in EAN.²³

Steady-State Fluorescence Measurement in Water.

Fluorescence measurements were also employed to further study the self-aggregation behavior of the alkylcarboxylate-based SAILs in water at 25 °C. The fluorescence emission spectrum of pyrene exhibits a character of five bands in the region of 370–400 nm. In a polar media, there exists an enhancement of the 0–0 band (peak 1) by a mechanism involving vibronic coupling, being similar to the Ham effect in the absorption spectra of benzene.⁴⁷ Thus, the intensity ratio of the first to the third vibronic peaks (I_1/I_3), dependent on the polarity of environment, can be used to analyze and obtain the cmc of surfactants in aqueous solution.^{48,49} Figure 7 shows the variation of the I_1/I_3 ratio with the concentration of the synthesized SAILs. The cmc values derived from the I_1/I_3 data

are listed in Table 1. It is clear that the data are in accordance with the cmc values obtained by the surface tension measurements.

Electrical Conductivity Measurement in Water. The concentration dependencies of the specific conductivity at different temperatures for $[C_4mim][C_nH_{2n-1}O_2]$ ($n = 8, 10, 12$) aqueous solutions are described in Figure 8. It is apparent that the gradual increase of the ionic liquid concentration leads to two linear fragments, and the steep change of slope is assigned to the cmc value of SAILs (shown in Table 1),⁵⁰ which are in agreement with the cmc values obtained by surface tension and fluorescence measurements at the same temperature. Based on the mixed electrolyte model of micellar solution developed by Shanks and Franes,⁵⁰ the degree of counterion binding (β) can also be estimated from the electrical conductivity versus concentration plots. The values of β for $[C_4mim][C_nH_{2n-1}O_2]$ ($n = 8, 10, 12$) at various temperatures are summarized in Table 2. Compared with the corresponding sodium salts of fatty acids, octoate ($\beta = 0.57$), decanoate ($\beta = 0.50$), laurate ($\beta = 0.35$),³⁵ the present SAILs have lower β values at 25 °C. This can be ascribed to the effect of smaller inorganic counterion (Na^+) and larger cyclic organic counterion ($[C_4mim]^+$). In addition, it is observed that all the alkylcarboxylate-based SAILs studied here have much smaller β values at 25 °C than the alkylsulfate-based SAILs with the same hydrophobic chain length. This discrepancy is primarily caused by the difference in the size of headgroups and the electrostatic repulsion between them. Compared with alkylsulfate-based SAILs, the less electro-negative anion of alkylcarboxylate-based SAILs leads to less C_4mim^+ counterions binding to the surface of micelles. However, the smaller steric hindrance strengthens the interaction between the imidazolium cation and headgroup of $C_nH_{2n-1}O_2^-$, resulting in more counterions existing at the micellar surface. The smaller values of β for $[C_4mim]-[C_nH_{2n-1}O_2]$ suggest that the electronegativity plays a dominant role over the size of headgroup.

Thermodynamics of Micellization Formation. According to the pseudophase model of micellization, micellar thermodynamic parameters were estimated. The standard Gibbs free energy of micellization (ΔG_m^θ), the micellization standard enthalpy (ΔH_m^θ), and the micellization standard entropy (ΔS_m^θ) can be estimated by the following equation

$$\Delta G_m^\theta = (1 + \beta)RT \ln X_{cmc} \quad (4)$$

$$\Delta H_m^\theta = -RT^2(1 + \beta)d \ln X_{cmc}/dT \quad (5)$$

$$\Delta S_m^\theta = (\Delta H_m^\theta - \Delta G_m^\theta)/T \quad (6)$$

where β is the degree of counterion binding of micelle, which can be obtained by ratio of the slopes of electrical conductivity versus concentration plots above and below cmc. For SAILs in EAN, we assign 1 to β .²² R is the ideal gas constant, T is the absolute temperature, and X_{cmc} is the cmc in molar fraction.

Based on the experimental results of surface tension and electrical conductivity measurements, the thermodynamic parameters of micellization processes for $[C_4mim][C_nH_{2n-1}O_2]$ ($n = 8, 10, 12$) are listed in Table 2, along with the data reported for $[C_4mim][C_nH_{2n-1}SO_4]$ ($n = 10, 12$).³³ The variation plots of these parameters as a function of temperature are described in Figures 9 and 10. The negative values of ΔG_m^θ mean that micellization of the studied SAILs in either water or EAN is a spontaneous process in the temperature range investigated. Moreover, the ΔG_m^θ values become more negative

Table 2. Thermodynamic Parameters Obtained for Micelle Formation of $[C_4mim][C_nH_{2n-1}O_2]$ ($n = 8, 10, 12$), Along with the Reported Data of $[C_4mim][C_nH_{2n+1}SO_4]$ ($n = 10, 12$) at Different Temperatures

	n	T (°C)	cmc (mM)		β	ΔC_m^θ (kJ/mol)		ΔH_m^θ (kJ/mol)		$-T\Delta S_m^\theta$ (kJ/mol)	
$[C_4\text{mim}][C_n\text{H}_{2n-1}\text{O}_2]$	8	25	44.9 ^a	51.8 ^b	0.13	-20.0 ^a	-35.1 ^b	-1.09 ^a	-12.0 ^b	-18.9 ^a	-23.1 ^b
		35	45.8	60.5	0.18	-21.4	-35.8	-1.21	-15.8	-20.2	-20.0
		45	46.0	65.1	0.17	-21.9	-36.3	-1.28	-21.2	-20.6	-15.1
		55	46.7	67.2	0.27	-24.6	-36.7	-1.48	-27.2	-23.1	-9.45
	10	25	3.55	29.9	0.29	-30.9	-37.8	-2.48	-12.4	-28.4	-25.4
		35	3.62	31.2	0.33	-32.8	-38.6	-2.73	-16.2	-30.1	-22.4
		45	3.68	33.3	0.47	-37.3	-39.2	-3.21	-19.1	-34.1	-20.1
		55	3.83	37.2	0.70	-44.4	-39.8	-4.41	-22.0	-40.0	-17.8
	12	25	0.45	10.5	0.07	-31.0	-42.9	-2.69	-20.8	-28.3	-22.1
		35	0.46	11.3	0.02	-30.6	-43.6	-2.74	-24.4	-27.9	-19.2
		45	0.48	13.4	0.10	-33.9	-44.6	-3.15	-28.7	-30.8	-15.4
		55	0.50	16.0	0.09	-34.6	-44.1	-3.32	-31.4	-31.3	-13.1
$[C_4\text{mim}][C_n\text{H}_{2n+1}\text{SO}_4]^c$	10	25	8.8		0.52	-33.1		-5.69		-27.4	
	12	25	1.9		0.65	-41.7		-5.05		-36.7	

^a $[C_4mim][C_nH_{2n-1}O_2]$ in water, from electrical conductivity measurements. ^b $[C_4mim][C_nH_{2n-1}O_2]$ in EAN, from surface tension measurements.^c $[C_4mim][C_nH_{2n+1}SO_4]$, reported in ref 33.

with the increase of the hydrophobic chain length, which is beneficial for the formation of micelles. At each temperature, the negative value of ΔG_m^θ for $[C_4mim][C_nH_{2n-1}O_2]$ in water is always larger than that in EAN, suggesting that it can form micelles easily in the former. All the ΔH_m^θ values are negative as well, indicating an exothermic micellization process in these two kinds of solvents. In water, the negative values of $(-T\Delta S_m^\theta)$ are much lower than those of ΔH_m^θ , indicating that the micellization for the SAILs is entropy-driven (Figure 9). This observation is consistent with the results for anionic SAILs, $[C_4mim][C_nH_{2n+1}SO_4]$ ($n = 10, 12$),³³ and cationic SAILs, $[C_nmim]Br$ ($n = 12, 14, 16$).⁵¹ During this process, the solvated water molecules are released, which results in an entropy increase.⁵² While in EAN (Figure 10), over the whole temperature range, the $-T\Delta S_m^\theta$ value always becomes more negative with the increase of temperature and intersects with the plot of ΔH_m^θ versus temperature. Before the intersection, the contribution of entropy to ΔG_m^θ is larger than that of enthalpy, while after the intersection, the enthalpy plays a major role in the determination of ΔG_m^θ . So the micelle formation in EAN is entropy-driven at low temperature and enthalpy-driven at high temperature. As is well-known, in aqueous media, the micellization of ionic surfactants is mainly contributed by hydrophobic effect around the hydrocarbon chains and electrostatic repulsion between ions.⁵³ The analogous mechanism of micelle formation can be proposed for $[C_4mim][C_nH_{2n-1}O_2]$ in EAN, which has a protic nature. There exists strong solvophobic solvation around the hydrophobic part of $[C_4mim][C_nH_{2n-1}O_2]$ molecule, caused by the hydrogen bond between NO_3^- of EAN and the proton on C-a of the imidazolium ring. The solvophobic solvation is similar to the hydrophobic effect in aqueous solution, where a hydrogen-bonding network around the hydrocarbon chain causes the hydrophobic effect.²¹ Meanwhile, the interaction between $CH_3CH_2NH_3^+$ and $[C_4mim]^+$ cations enhances the electrostatic repulsion of the SAILs. These two reasons can contribute to the negative enthalpy change. In addition, as compared with $[C_4mim][C_nH_{2n+1}SO_4]$ ($n = 10, 12$),³³ the negative value of ΔG_m^θ of the corresponding alkylcarboxylate-based SAILs is much lower, suggesting an easy micelle formation (i.e., a lower cmc).

¹H NMR Spectra for $[C_4mim][C_{10}H_{19}O_2]$ in Water. ¹H NMR, a sensitive and accurate technique, was also used to investigate the aggregation behavior of alkylcarboxylate-based SAILs in water at 25 °C. As a typical example, the variation of the chemical shift, $\Delta\delta(\Delta\delta = \delta_{obs} - \delta_{mon})$, as a function of reciprocal concentration for protons H_b , H_i on $[C_4mim][C_{10}H_{19}O_2]$, is depicted in Figure 11. A slight change of the chemical shifts is observed below cmc. At cmc, the sharp change of chemical shifts appears, indicating the change of microenvironment, related to the formation of micelles.²³ It can be seen that the cmc value (about 3.5 mM) obtained by ¹H NMR is in close agreement with that obtained by other measurements at 25 °C (Table 1). The magnitude changes for $\Delta\delta$ are generally affected by the medium effect, aromatic ring current, hydrogen bond, and conformation effect.⁵⁴ The downfield shift of the H_b upon micellization can be ascribed to medium effect, from water to micelle, a nonpolar medium. Another reason mainly results from the deshielding effect. As the imidazole ring has a quite rigorous geometrical restriction, protons located in the field of the ring are substantially shifted due to the ring-current effect. In addition, electron density of these protons on imidazolium cation is reduced due to contact with electronegative oxygen atom of the anionic headgroup (formation of hydrogen bonding). Protons on the anion chain show an upfield shift in aggregates formation. It is known that partial changeover from *trans* to *gauche* conformation for alkyl chains can cause an upfield shift.⁵⁵ The aromatic ring-induced shielding effect can also lead to an upfield shift.⁵⁶ H_i has an obvious change of chemical shift because it is close to the imidazolium cation during the formation of micelles.

DFT Calculation. To qualitatively understand the interactions of alkylcarboxylate-based SAILs with water or EAN, which affects their aggregation behavior significantly, we used quantum chemistry calculations for further study. We optimized the structures of the isolated $[C_4mim][C_nH_{2n-1}O_2]$ ($n = 8, 10, 12$), EAN, and H₂O, respectively, along with the (1:1) binary complexes of SAILs with EAN and H₂O. Figure 12 shows the optimized geometries of the complex system, and Table 3 lists the interaction energy (E_{int}), calculated by the stabilization energy difference between complexes and monomers. As seen in Table 3, the calculated interaction energy of the SAILs–EAN complex is larger than that of SAILs–H₂O.

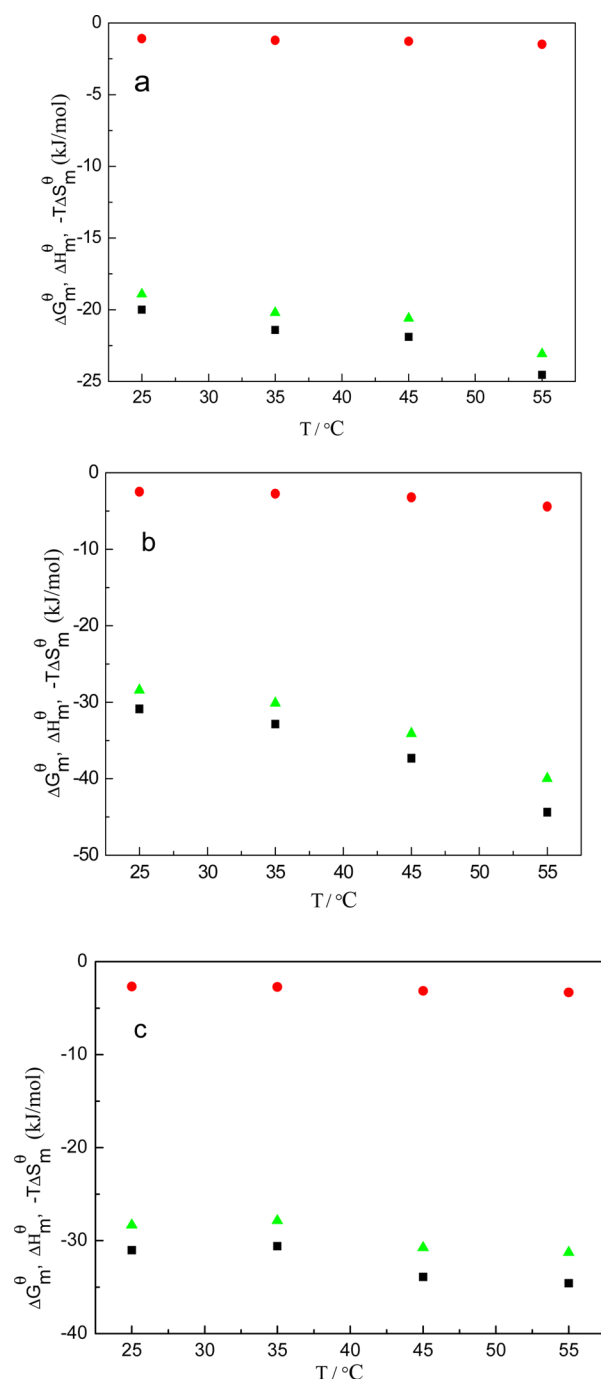


Figure 9. Plots of the thermodynamic parameters of micelle formation against T for $[C_4mim][C_nH_{2n-1}O_2]$ in water: (a) $n = 8$; (b) $n = 10$; (c) $n = 12$. Squares, circles, and triangles represent ΔG_m^θ , ΔH_m^θ , and $-T\Delta S_m^\theta$, respectively.

The primary reason behind this stronger interaction for EAN system is the strong hydrogen bonding between COO^-NH as evidenced from the distance (1.56 \AA),^{57,58} which is shown in Figure 12. This implies the stabilization of the SAILs–EAN complex. Strong interaction with EAN causes a large increase in cmc value.^{57–59} This supports our observation made from the surface tension measurements.

CONCLUSIONS

In this work, new alkylcarboxylate-based SAILs $[C_4mim]-[C_nH_{2n-1}O_2]$ ($n = 8, 10, 12$) were simply synthesized via

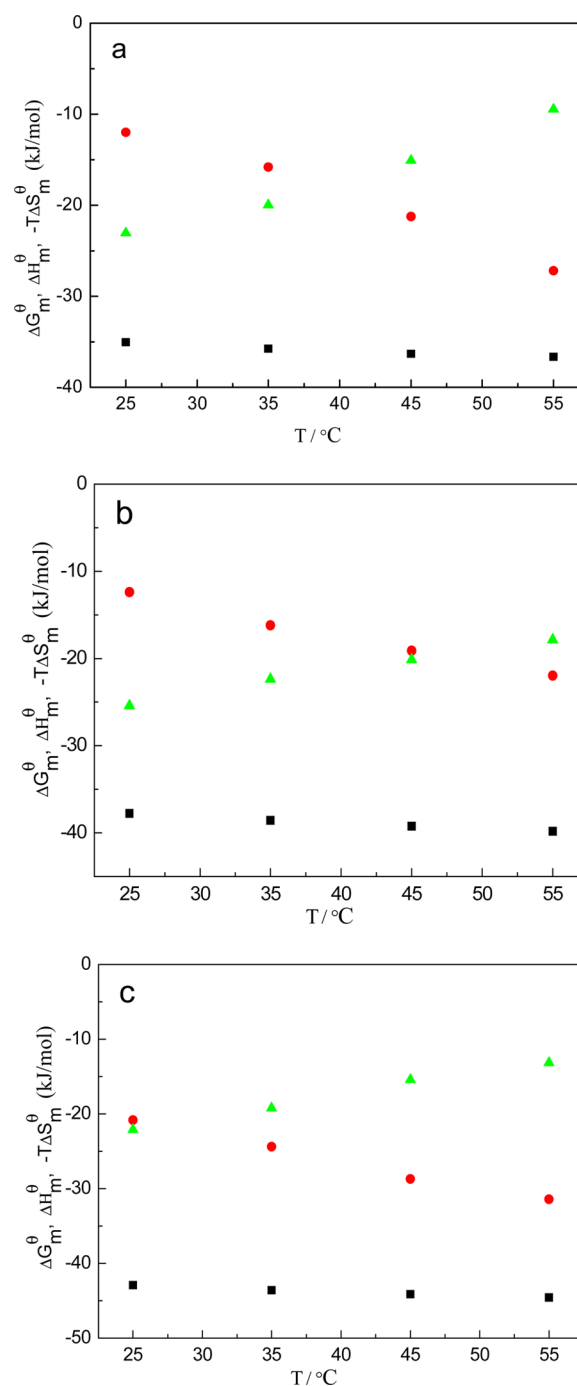


Figure 10. Plots of the thermodynamic parameters of micelle formation against temperature for $[C_4mim][C_nH_{2n-1}O_2]$ in EAN: (a) $n = 8$; (b) $n = 10$; (c) $n = 12$. Squares, circles, and triangles represent ΔG_m^θ , ΔH_m^θ , and $-T\Delta S_m^\theta$, respectively.

neutralization reactions. They can be readily generated from commercially available, cheap starting materials, with lower potential environmental hazards (halogen free) than normal imidazolium-based SAILs. Their aggregation behavior in both water and EAN has been investigated. The cmc value of $[C_4mim][C_nH_{2n-1}O_2]$ in water obtained by various methods shows fairly good agreement. By comparison, $[C_4mim]-[C_nH_{2n-1}O_2]$ display a higher ability to aggregate in water than the corresponding traditional anionic surfactants, SAC, and anionic SAILs, $[C_4mim][C_nH_{2n+1}SO_4]$. Quantum chemistry calculation results show that the less electronegativity of

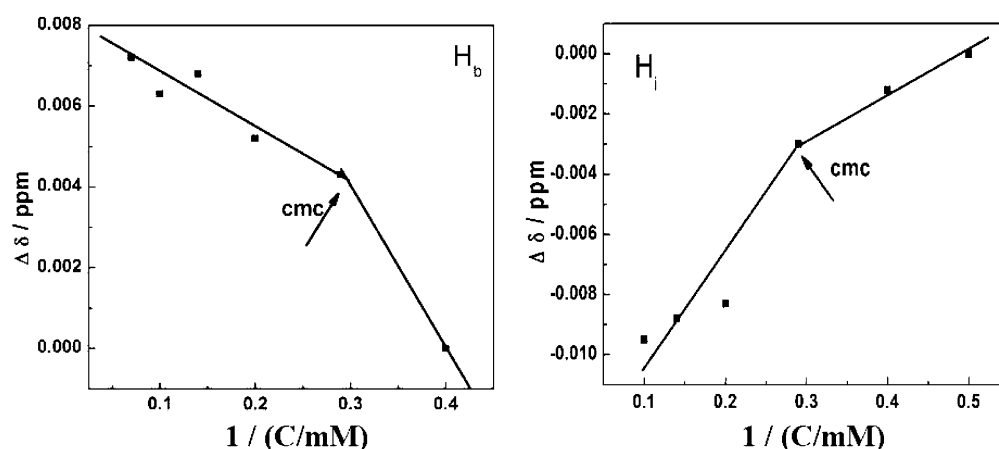


Figure 11. Variation of chemical shift for protons H_b , H_i on $[C_4mim][C_{10}H_{19}O_2]$ versus the reciprocal concentration in D_2O at 25 °C.

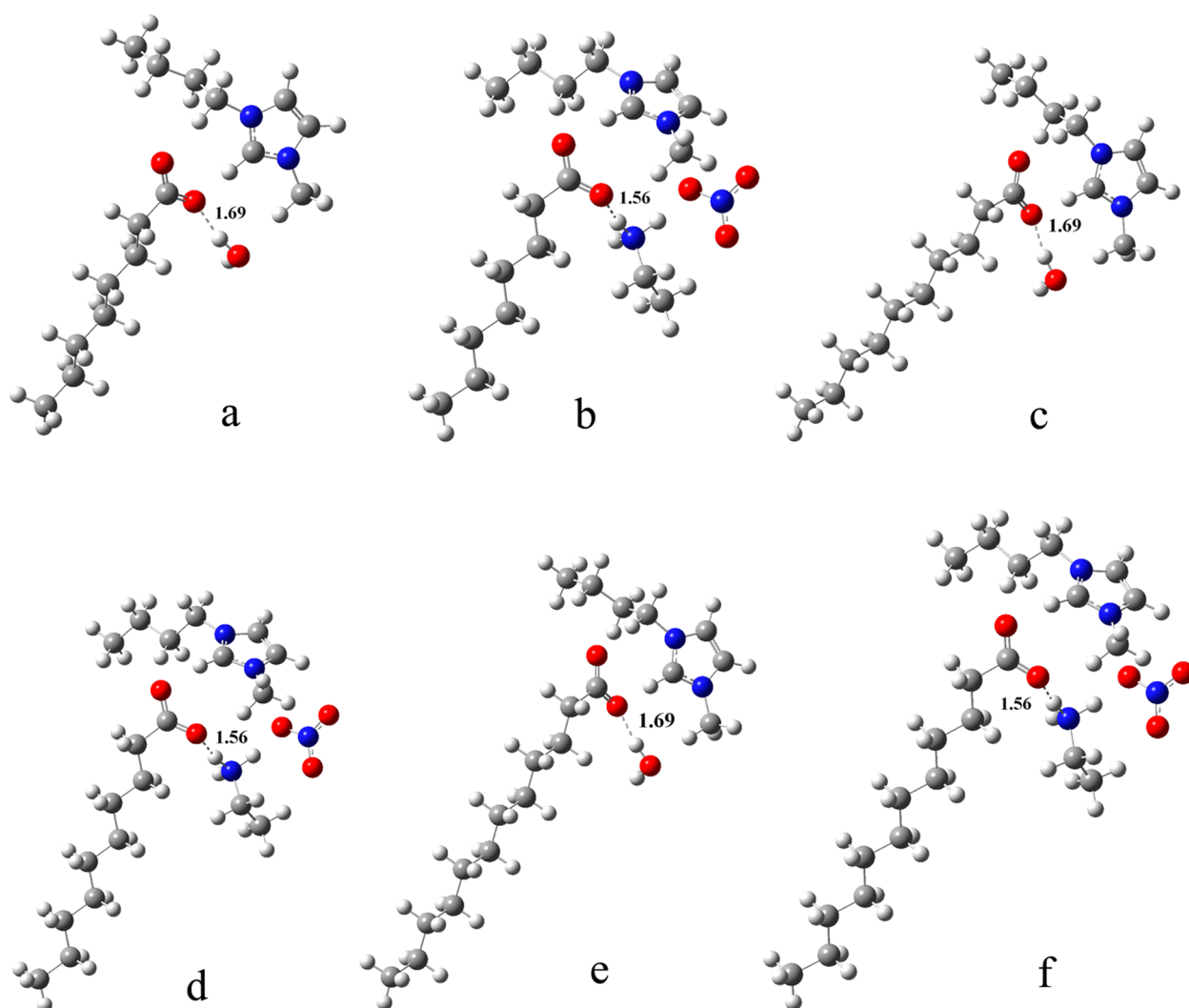


Figure 12. Geometries optimized at the B3LYP/6-31G(d, p) level: (a) $[C_4mim][C_8H_{15}O_2]-H_2O$, (b) $[C_4mim][C_8H_{15}O_2]-EAN$, (c) $[C_4mim][C_{10}H_{19}O_2]-H_2O$, (d) $[C_4mim][C_{10}H_{19}O_2]-EAN$, (e) $[C_4mim][C_{12}H_{23}O_2]-H_2O$, (f) $[C_4mim][C_{12}H_{23}O_2]-EAN$. Color code for atoms: blue, nitrogen; red, oxygen; dark gray, carbon; light gray, hydrogen.

the polar headgroup of $[C_4mim][C_nH_{2n-1}O_2]$ is mainly responsible for its cmc, which is lower than that of $[C_4mim][C_nH_{2n+1}SO_4]$. The micelle formation for the synthesized SAILs in EAN is more difficult than that in water. The thermodynamic analysis on the micellization

process of $[C_4mim][C_nH_{2n-1}O_2]$ shows that the micelle formation is entropy-driven in water through the whole temperature range investigated and entropy-driven at low temperature and enthalpy-driven at high temperature in EAN. DFT calculation indicates that the SAILs–EAN system has a

Table 3. Interaction Energy ($-E_{\text{int}}$) of $[\text{C}_4\text{mim}][\text{C}_n\text{H}_{2n-1}\text{O}_2]$ with H_2O (a) and EAN (b)

SAILs	interaction energy ($-E_{\text{int}}/\text{kJ}\cdot\text{mol}^{-1}$)	
$[\text{C}_4\text{mim}][\text{C}_8\text{H}_{15}\text{O}_2]$	71.41 ^a	101.40 ^b
$[\text{C}_4\text{mim}][\text{C}_{10}\text{H}_{19}\text{O}_2]$	71.38 ^a	101.44 ^b
$[\text{C}_4\text{mim}][\text{C}_{12}\text{H}_{23}\text{O}_2]$	70.98 ^a	101.13 ^b

larger stabilization than the SAILs–water system due to the formation of hydrogen bonding, resulting in a higher cmc value in EAN. The obtained results can make up for the study of aggregation behavior for the environmentally benign alkylcarboxylate-based SAILs and lay a foundation for their potential applications in various fields, including colloid and interface, nanomaterials synthesis, and so forth.

AUTHOR INFORMATION

Corresponding Author

*E-mail: ylmilt@sdu.edu.cn. Fax: +86-531-88564750. Tel.: +86-531-88364807.

Notes

The authors declare no competing financial interest.

ACKNOWLEDGMENTS

This work was supported by the National Natural Science Foundation of China (no. 21373128), the Natural Science Foundation of Shandong Province of China (no. ZR2011BM017) and the R&D Project of Shengli Oilfield of Sinopec (no.30200019-13-ZC0613-0046).

REFERENCES

- (1) Rogers, R. D.; Seddon, K. R. Ionic Liquids–Solvents of the Future? *Science* **2003**, 302, 792–793.
- (2) Anouti, M.; Sizaret, P.-Y.; Ghimbeu, C.; Galiano, H.; Lemordant, D. Physicochemical Characterization of Vesicles Systems Formed in Mixtures of Protic Ionic Liquids and Water. *Colloids Surf., A* **2012**, 395, 190–198.
- (3) Wang, H.; Wang, J.; Zhang, S.; Xuan, X. Structural Effects of Anions and Cations on the Aggregation Behavior of Ionic Liquids in Aqueous Solutions. *J. Phys. Chem. B* **2008**, 112, 16682–16689.
- (4) Wang, X.; Yu, L.; Jiao, J.; Zhang, H.; Wang, R.; Chen, H. Aggregation Behavior of COOH-Functionalized Imidazolium-Based Surface Active Ionic Liquids in Aqueous Solution. *J. Mol. Liq.* **2012**, 173, 103–107.
- (5) Anouti, M.; Jones, J.; Boisset, A.; Jacquemin, J.; Caillon-Caravanier, M.; Lemordant, D. Aggregation Behavior in Water of New Imidazolium and Pyrrolidinium Alkylcarboxylates Protic Ionic Liquids. *J. Colloid Interface Sci.* **2009**, 340, 104–111.
- (6) Srinivasa Rao, K.; Singh, T.; Trivedi, T. J.; Kumar, A. Aggregation Behavior of Amino Acid Ionic Liquid Surfactants in Aqueous Media. *J. Phys. Chem. B* **2011**, 115, 13847–13853.
- (7) Singh, T.; Kumar, A. Aggregation Behavior of Ionic Liquids in Aqueous Solutions: Effect of Alkyl Chain Length, Cations, and Anions. *J. Phys. Chem. B* **2007**, 111, 7843–7851.
- (8) Wang, J.; Zhang, L.; Wang, H.; Wu, C. Aggregation Behavior Modulation of 1-Dodecyl-3-methylimidazolium Bromide by Organic Solvents in Aqueous Solution. *J. Phys. Chem. B* **2011**, 115, 4955–4962.
- (9) Singh, T.; Drechsler, M.; Mueller, A. H. E.; Mukhopadhyay, L.; Kumar, A. Micellar Transitions in the Aqueous Solutions of a Surfactant-Like Ionic Liquid: 1-Butyl-3-Methylimidazolium Octylsulfate. *Phys. Chem. Chem. Phys.* **2010**, 12, 11728–11735.
- (10) Blesic, M.; Lopes, A. N.; Melo, E.; Petrovski, Z.; Plechkova, N. V.; Canongia Lopes, J. N.; Seddon, K. R.; Rebelo, L. S. P. N. On the Self-Aggregation and Fluorescence Quenching Aptitude of Surfactant Ionic Liquids. *J. Phys. Chem. B* **2008**, 112, 8645–8650.

(11) Brown, P.; Butts, C.; Dyer, R.; Eastoe, J.; Grillo, I.; Guittard, F. d. R.; Rogers, S.; Heenan, R. Anionic Surfactants and Surfactant Ionic Liquids with Quaternary Ammonium Counterions. *Langmuir* **2011**, 27, 4563–4571.

(12) Brown, P.; Butts, C. P.; Eastoe, J.; Fermin, D.; Grillo, I.; Lee, H.-C.; Parker, D.; Plana, D.; Richardson, R. M. Anionic Surfactant Ionic Liquids with 1-Butyl-3-Methyl-Imidazolium Cations: Characterization and Application. *Langmuir* **2012**, 28, 2502–2509.

(13) Zech, O.; Thomaier, S.; Bauduin, P.; Rück, T.; Touraud, D.; Kunz, W. Microemulsions with an Ionic Liquid Surfactant and Room Temperature Ionic Liquids as Polar Pseudo-Phase. *J. Phys. Chem. B* **2008**, 113, 465–473.

(14) Zhao, Y.; Chen, X.; Wang, X. Liquid Crystalline Phases Self-Organized from a Surfactant-like Ionic Liquid $\text{C}_{16}\text{mimCl}$ in Ethylammonium Nitrate. *J. Phys. Chem. B* **2009**, 113, 2024–2030.

(15) Zhao, Y.; Chen, X.; Jing, B.; Wang, X.; Ma, F. Novel Gel Phase Formed by Mixing a Cationic Surfactive Ionic Liquid $\text{C}_{16}\text{mimCl}$ and an Anionic Surfactant SDS in Aqueous Solution. *J. Phys. Chem. B* **2009**, 113, 983–988.

(16) Singh, T.; Kumar, A. Self-Aggregation of Ionic Liquids in Aqueous Media: a Thermodynamic Study. *Colloids Surf., A* **2008**, 318, 263–268.

(17) Inoue, T.; Ebina, H.; Dong, B.; Zheng, L. Electrical Conductivity Study on Micelle Formation of Long-Chain Imidazolium Ionic Liquids in Aqueous Solution. *J. Colloid Interface Sci.* **2007**, 314, 236–241.

(18) Łuczak, J.; Jungnickel, C.; Joskowska, M.; Thöming, J.; Hupka, J. Thermodynamics of Micellization of Imidazolium Ionic Liquids in Aqueous Solutions. *J. Colloid Interface Sci.* **2009**, 336, 111–116.

(19) Thomaier, S.; Kunz, W. Aggregates in Mixtures of Ionic Liquids. *J. Mol. Liq.* **2007**, 130, 104–107.

(20) Evans, D. F.; Chen, S.-H.; Schriver, G. W.; Arnett, E. M. Thermodynamics of Solution of Nonpolar Gases in a Fused Salt. Hydrophobic Bonding Behavior in a Nonaqueous System. *J. Am. Chem. Soc.* **1981**, 103, 481–482.

(21) Kang, W.; Dong, B.; Gao, Y.; Zheng, L. Aggregation Behavior of Long-Chain Imidazolium Ionic Liquids in Ethylammonium Nitrate. *Colloid Polym. Sci.* **2010**, 288, 1225–1232.

(22) Shi, L.; Zhao, M.; Zheng, L. Micelle Formation By N-Alkyl-N-Methylpyrrolidinium Bromide in Ethylammonium Nitrate. *Colloids Surf., A* **2011**, 392, 305–312.

(23) Jiao, J.; Dong, B.; Zhang, H.; Zhao, Y.; Wang, X.; Wang, R.; Yu, L. Aggregation Behaviors of Dodecyl Sulfate-Based Anionic Surface Active Ionic Liquids in Water. *J. Phys. Chem. B* **2012**, 116, 958–965.

(24) Harjani, J. R.; Singer, R. D.; Garcia, M. T.; Scammells, P. J. Biodegradable Pyridinium Ionic Liquids: Design, Synthesis and Evaluation. *Green Chem.* **2009**, 11, 83–90.

(25) Trivedi, T. J.; Rao, K. S.; Singh, T.; Mandal, S. K.; Sutradhar, N.; Panda, A. B.; Kumar, A. Task-Specific, Biodegradable Amino Acid Ionic Liquid Surfactants. *ChemSusChem* **2011**, 4, 604–608.

(26) Brown, P.; Butts, C. P.; Eastoe, J.; Grillo, I.; James, C.; Khan, A. New Catanionic Surfactants with Ionic Liquid Properties. *J. Colloid Interface Sci.* **2013**, 395, 185–189.

(27) Zhuo, K.; Chen, Y.; Chen, J.; Bai, G.; Wang, J. Interactions of 1-Butyl-3-Methylimidazolium Carboxylate Ionic Liquids with Glucose in Water: A Study of Volumetric Properties, Viscosity, Conductivity and NMR. *Phys. Chem. Chem. Phys.* **2011**, 13, 14542–14549.

(28) Fukaya, Y.; Sugimoto, A.; Ohno, H. Superior Solubility of Polysaccharides in Low Viscosity, Polar, and Halogen-Free 1,3-Dialkylimidazolium Formates. *Biomacromolecules* **2006**, 7, 3295–3297.

(29) Anderson, J. L.; Pino, V.; Hagberg, E. C.; Sheares, V. V.; Armstrong, D. W. Surfactant Solvation Effects and Micelle Formation in Ionic Liquids. *Chem. Commun.* **2003**, 2444–2445.

(30) Hao, J.; Song, A.; Wang, J.; Chen, X.; Zhuang, W.; Shi, F.; Zhou, F.; Liu, W. Self-Assembled Structure in Room-Temperature Ionic Liquids. *Chem.—Eur. J.* **2005**, 11, 3936–3940.

(31) Fletcher, K. A.; Pandey, S. Surfactant Aggregation within Room-Temperature Ionic Liquid 1-Ethyl-3-Methylimidazolium Bis-(trifluoromethylsulfonyl)imide. *Langmuir* **2003**, 20, 33–36.

- (32) Evans, D. F.; Yamauchi, A.; Roman, R.; Casassa, E. Z. Micelle Formation in Ethylammonium Nitrate, a Low-Melting Fused Salt. *J. Colloid Interface Sci.* **1982**, *88*, 89–96.
- (33) Jiao, J.; Han, B.; Lin, M.; Cheng, N.; Yu, L.; Liu, M. Salt-Free Catanionic Surface Active Ionic Liquids 1-Alkyl-3-Methylimidazolium Alkylsulfate: Aggregation Behavior in Aqueous Solution. *J. Colloid Interface Sci.* **2013**, *412*, 24–30.
- (34) Campbell, A. N.; Lakshminarayanan, G. R. Conductances and Surface Tensions of Aqueous Solutions of Sodium Decanoate, Sodium Laurate, and Sodium Myristate, at 25° and 35°. *Can. J. Chem.* **1965**, *43*, 1729–1737.
- (35) Frisch, M. J.; Trucks, G. W.; Schlegel, H. B.; Scuseria, G. E.; Robb, M. A.; Cheeseman, J. R.; Scalmani, G.; Barone, V.; Mennucci, B.; Petersson, G. A.; et al. *Gaussian 09*, revision A.02; Gaussian, Inc.: Wallingford, CT, 2009.
- (36) Becke, A. D. Density-Functional Thermochemistry. III: The Role of Exact Exchange. *J. Chem. Phys.* **1993**, *98*, 5648–5652.
- (37) Lee, C.; Yang, W.; Parr, R. G. Development of the Colle-Salvetti Correlation-Energy Formula into a Functional of the Electron Density. *Phys. Rev. B* **1988**, *37*, 785–789.
- (38) Barić, D.; Maksić, Z. B. Atomic Additivity of the Correlation Energy in Molecules by the DFT-B3LYP Scheme. *J. Phys. Chem. A* **2003**, *107*, 11577–11586.
- (39) Hehre, W. J.; Ditchfield, R.; Pople, J. A. Self-Consistent Molecular Orbital Methods. XII. Further Extensions of Gaussian-Type Basis Sets for Use in Molecular Orbital Studies of Organic Molecules. *J. Chem. Phys.* **1972**, *56*, 2257–2261.
- (40) Martell, J. M.; Goddard, J. D.; Eriksson, L. A. Assessment of Basis Set and Functional Dependencies in Density Functional Theory: Studies of Atomization and Reaction Energies. *J. Phys. Chem. A* **1997**, *101*, 1927–1934.
- (41) Rosen, M. J. *Surfactants and Interfacial Phenomena*, 2nd ed.; Wiley: New York, 1989.
- (42) Miki, K.; Westh, P.; Nishikawa, K.; Koga, Y. Effect of an “Ionic Liquid” Cation, 1-Butyl-3-Methylimidazolium, on the Molecular Organization of H₂O. *J. Phys. Chem. B* **2005**, *109*, 9014–9019.
- (43) Jaycock, M. J.; Parfitt, G. D. *Chemistry of Interfaces*; John Wiley and Sons: New York, 1981.
- (44) Bondi, A. van der Waals Volumes and Radii. *J. Phys. Chem.* **1964**, *68*, 441–451.
- (45) Kleven, H. B. Structure and Aggregation in Dilute Solution of Surface Active Agents. *J. Am. Oil Chem. Soc.* **1953**, *30*, 74–80.
- (46) Lu, F.; Shi, L.; Gu, Y.; Yang, X.; Zheng, L. Aggregation Behavior of Alkyl Triphenyl Phosphonium Bromides in Aprotic and Protic Ionic Liquids. *Colloid Polym. Sci.* **2013**, *291*, 2375–2384.
- (47) Koyanagi, M. Effect of Dispersion Forces of Solvents II. On the O-O band of the Near Ultraviolet Absorption Spectrum of Benzene in Fluid Solutions. *J. Mol. Spectrosc.* **1968**, *25*, 273–290.
- (48) Kalyanasundaram, K.; Thomas, J. K. Environmental Effects on Vibronic Band Intensities in Pyrene Monomer Fluorescence and Their Application in Studies of Micellar Systems. *J. Am. Chem. Soc.* **1977**, *99*, 2039–2044.
- (49) Dong, B.; Zhao, X.; Zheng, L.; Zhang, J.; Li, N.; Inoue, T. Aggregation Behavior of Long-chain Imidazolium Ionic Liquids in Aqueous Solution: Micellization and Characterization of Micelle Microenvironment. *Colloids Surf., A* **2008**, *317*, 666–672.
- (50) Shanks, P. C.; Franes, E. I. Estimation of Micellization Parameters of Aqueous Sodium Dodecyl Sulfate from Conductivity Data. *J. Phys. Chem.* **1992**, *96*, 1794–1805.
- (51) Geng, F.; Liu, J.; Zheng, L.; Yu, L.; Li, Z.; Li, G.; Tung, C. Micelle Formation of Long-Chain Imidazolium Ionic Liquids in Aqueous Solution Measured by Isothermal Titration Microcalorimetry. *J. Chem. Eng. Data* **2010**, *55*, 147–151.
- (52) Tanford, C. *The Hydrophobic Effect: Formation of Micelles and Biological Membranes*, 2nd ed.; Wiley: New York, 1980.
- (53) Muller, N. Temperature Dependence of Critical Micelle Concentrations and Heat Capacities of Micellization for Ionic Surfactants. *Langmuir* **1993**, *9*, 96–100.
- (54) Deng, M.; Huang, X.; Wu, R.; Wang, Y. Micellization-Induced Conformational Change of a Chiral Proline Surfactant. *J. Phys. Chem. B* **2008**, *112*, 10509–10513.
- (55) Singh, T.; Kumar, A. Aggregation Behavior of Ionic Liquids in Aqueous Solutions: Effect of Alkyl Chain Length, Cations, and Anions. *J. Phys. Chem. B* **2007**, *111*, 7843–7851.
- (56) Okano, L. T.; Seoud, O. A. E.; Halstead, T. K. Proton NMR Study on Aggregation of Cationic Surfactants in Water: Effects of the Structure of the Headgroup. *Colloid Polym. Sci.* **1997**, *275*, 138–145.
- (57) Weimann, M.; Fárnik, M.; Suhm, M. A.; Alikhani, M. E.; Sadlej, J. Cooperative and Anticooperative Mixed Micelles of HCl and Methanol. *J. Mol. Struct.* **2006**, *790*, 18–26.
- (58) Das, D.; Dey, J.; Chandra, A. K.; Thapa, U.; Ismail, K. Aggregation Behavior of Sodium Dioctylsulfosuccinate in Aqueous Ethylene Glycol Medium. A Case of Hydrogen Bonding between Surfactant and Solvent and Its Manifestation in the Surface Tension Isotherm. *Langmuir* **2012**, *28*, 15762–15769.
- (59) Pan, A.; Mati, S. S.; Naskar, B.; Bhattacharya, S. C.; Moulik, S. P. Self-Aggregation of MEGA-9 (N-Nonanoyl-N-methyl-D-glucamine) in Aqueous Medium: Physicochemistry of Interfacial and Solution Behaviors with Special Reference to Formation Energetics and Micelle Microenvironment. *J. Phys. Chem. B* **2013**, *117*, 7578–7592.